JOURNAL OF VIROLOGY, Feb. 2007, p. 1140–1147 Vol. 81, No. 3
0022-538X/07/$08.00+0 doi:10.1128/JVI.01345-06


# Vaccinia Virus Interactions with the Cell Membrane Studied by New Chromatic Vesicle and Cell Sensor Assays▽

Z. Orynbayeva,[1] S. Kolusheva,[1] N. Groysman,[1] N. Gavrielov,[2] L. Lobel,[2] and R. Jelinek[1]*

*Department of Chemistry and Ilse Katz Center for Nanotechnology,[1] and Department of Virology,[2] Ben Gurion University of the Negev, Beer Sheva, Israel 84105*

Received 26 June 2006/Accepted 6 November 2006

**The potential danger of cross-species viral infection points to the significance of understanding the contributions of nonspecific membrane interactions with the viral envelope compared to receptor-mediated uptake as a factor in virus internalization and infection. We present a detailed investigation of the interactions of vaccinia virus particles with lipid bilayers and with epithelial cell membranes using newly developed chromatic biomimetic membrane assays. This analytical platform comprises vesicular particles containing lipids interspersed within reporter polymer units that emit intense fluorescence following viral interactions with the lipid domains. The chromatic vesicles were employed as membrane models in cell-free solutions and were also incorporated into the membranes of epithelial cells, thereby functioning as localized membrane sensors on the cell surface. These experiments provide important insight into membrane interactions with and fusion of virions and the kinetic profiles of these processes. In particular, the data emphasize the significance of cholesterol/sphingomyelin domains (lipid rafts) as a crucial factor promoting bilayer insertion of the viral particles. Our analysis of virus interactions with polymer-labeled living cells exposed the significant role of the epidermal growth factor receptor in vaccinia virus infectivity; however, the data also demonstrated the existence of additional non-receptor-mediated mechanisms contributing to attachment of the virus to the cell surface and its internalization.**

The essential initial step in the viral infection process involves transport of the virus or its genetic components through the host cell membrane. Membrane interactions and penetration of viral particles are generally complex multistep processes determined by varied factors and molecular events that have been elucidated for only a few viral species. Indeed, revealing the mechanisms of membrane binding by viral particles, bilayer fusion with the viral coat, and eventual virus internalization into the host cell is critical for understanding viral infection and propagation. In particular, determining the contributions of virus-lipid interactions to cell entry (rather than receptor-mediated uptake) is essential for gaining insight into the factors affecting cross-species infectivity.

*Vaccinia virus* (VV) is a member of the *Poxviridae* family, which coinfect a wide variety of mammalian cells. The two infectious forms of vaccinia virions include the intracellular mature virus (IMV) and the extracellular enveloped virus (EEV), which are structurally distinct and exhibit different biological features (1). The IMV is a single-enveloped particle containing different viral proteins on its membrane (18) and represents the majority of infectious progeny produced in cells and responsible for virus proliferation among neighboring cells. EEV has an additional outer membrane with specific proteins and corresponds to infecting distant cells (39). The precise mechanisms of VV entry into host cells have not been fully determined. Previous studies point to the occurrence of fusion between VV and the plasma membrane (2, 7, 20); however, it is not clear whether the viral membrane directly fuses with the cell membrane or whether the process is mediated by viral envelope proteins. Furthermore, even though it is generally assumed that initial virus binding is mediated through specific cell surface receptors, it has been reported that IMV and EEV particles bind to different receptors (44) and that IMV could recognize several principal receptors (8, 11, 19, 45). Overall, it is becoming increasingly evident that parallel mechanisms probably exist for recipient cell invasion, allowing VV to infect a wide range of host cells.

Herein we analyze membrane interactions of VV using a newly developed biomimetic platform comprising vesicular particles of lipids and the chromatic lipid-like polymer polydiacetylene (PDA) (35). Figure 1 depicts the principle of the lipid/PDA vesicle assay for studying membrane interactions. The mixed vesicles comprise both lipid domains, constituting the biomimetic membrane platform interspersed within the PDA matrix that functions as the chromatic reporter for the biological events occurring within the membrane (25). Interactions of viral particles with the lipid/PDA vesicles induce chromatic transformations within the polymer matrix, and analysis of those transformations yield biophysical information on events occurring within the membrane bilayers.

Conjugated PDA assemblies exhibit unique spectroscopic properties. PDA vesicular aggregates and films have been previously shown to undergo distinct blue-red colorimetric changes due to conformational transitions in the conjugated (ene-yne) polymer backbone, induced by external structural perturbations (9, 30, 35). The colorimetric transitions of PDA go hand in hand with unique fluorescence properties: no fluorescence is emitted by the initially polymerized blue-phase PDA, while the red-phase PDA strongly fluoresces at 560 nm and at 640 nm (24). The chromatic transformations of PDA

* Corresponding author. Mailing address: Department of Chemistry, Ben Gurion University, Beer Sheva, Israel 84103. Phone: 972-8-6461747. Fax: 972-8-6472943. E-mail: razj@bgu.ac.il.

▽ Published ahead of print on 15 November 2006.

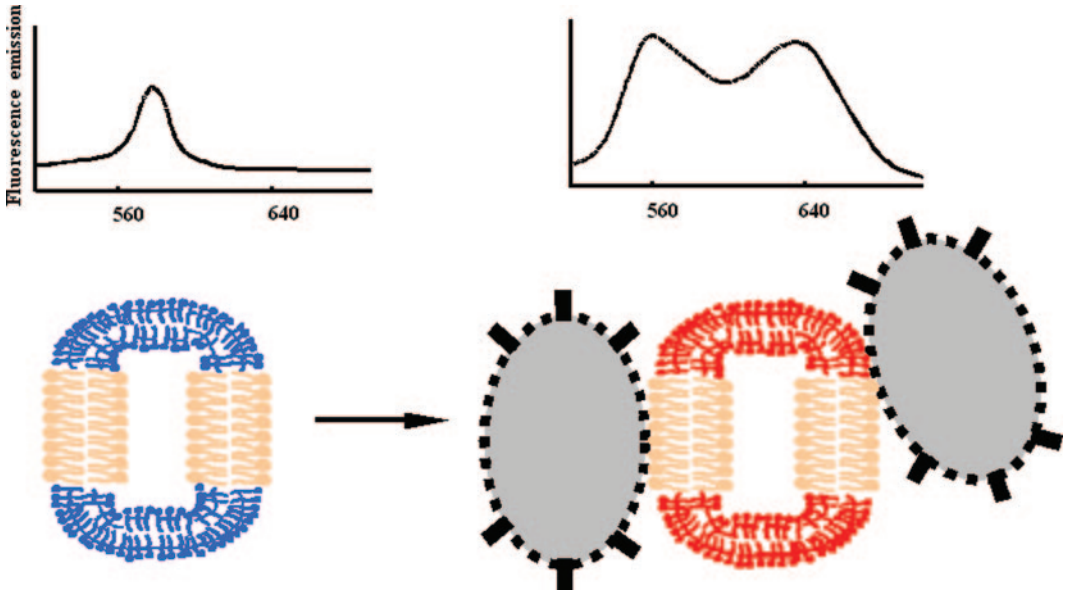


FIG. 1. Schematic depiction of the chromatic vesicle detection method. (Left) Unperturbed blue (nonfluorescent) vesicles (lipids [beige]; PDA [blue]); (right) viral particles (IMV) bind to the lipid/PDA vesicle, inducing transformation into the red (fluorescent) polymer phase.

also occur in biological contexts: recent studies have demonstrated that the blue-red and fluorescence transitions can be induced by amphiphilic and membrane-active molecules in vesicle assemblies comprising phospholipids incorporated within the PDA matrixes (22, 27, 37) and in PDA nanopatches attached to the surfaces of cells (31, 38). In such assemblies, interactions of biological analytes with the lipid bilayer domains gave rise to blue-red transitions and fluorescence induction from the PDA matrix. Among the important advantages of the lipid/PDA system for studying membrane processes is the feasibility of incorporating different lipid constituents in the vesicles for evaluating the contribution of lipid composition toward membrane binding and penetration (27).

Here we employ lipid/PDA vesicles and PDA-labeled epithelial cells for a systematic investigation of vaccinia virus interactions with membranes and to evaluate the significance of lipid interactions to virus internalization into the host cell. The results of chromatic analysis, together with the results of complementary biophysical techniques, demonstrate that interaction and fusion of IMV with plasma membrane lipids is an important process and possibly critical for viral internalization. Furthermore, we show that VV insertion into the membrane is highly dependent upon the presence of sphingomyelin (Sph)/cholesterol (Chl) domains (lipid rafts) in the cell membrane. The analysis further examines the role of the epidermal growth factor (EGF) receptor in promoting viral internalization and demonstrates that EGF receptor-mediated binding is not exclusive in affecting VV entry.

## MATERIALS AND METHODS

**Reagents.** The diacetylenic monomer 10,12-tricosadiynoic acid was obtained from GFS Chemicals (Powell, OH). Dimyristoylphosphatidylethanoleamine (DMPE), Sph, Chl, dimyristoylphosphatidylglycerol (DMPG), dimyristoylphosphatidylcholine (DMPC), and epidermal growth factor (human, recombinant) were purchased from Sigma-Aldrich. *N*-(7-Nitro-2,1,3-benzoxadiazol-4-yl) phosphatidylethanolamine (*N*-NBD-PE), *N*-(lissamine rhodamine B sulfonyl) phosphatidylethanolamine (*N*-Rh-PE), and *N*-[[4-(6-phenyl-1,3,5-hexatrienyl)phenyl] propyl] trimethylammonium-*p*-toluenesulfonate (TMAP-DPH) were obtained from Molecular Probes (Eugene, OR).

**Cells and virus.** CHO cells were maintained in F-12 (Ham) medium supplemented with 10% fetal calf serum, 2 mM L-glutamine, and 1% penicillin-streptomycin. The vaccinia virus Lister strain was used in all experiments. Viral stocks were grown and titrated on BSC-1 cells in stationary phase. Forty-eight hours after infection, the cells were harvested, and a cell pellet was obtained by centrifugation. The virus was released from the membranes by freeze-thaw cycles repeated three times followed by probe ultrasonication. This preparation was frozen at −80°C and used as a crude viral stock. We purified the IMV particles by the method of Joklik (21). Briefly, the crude stock was resuspended in10 mM Tris-HCl (pH 9) and passed 20 times through a 23-gauge needle. The nuclei and cell debris were then removed from the cell extracts by centrifugation (1,000 × *g*, 10 min, 20°C), followed by sedimentation (35,000 × *g*, 80 min, 20°C) through sucrose cushion (36% [wt/vol] in 1 mM $NaH_2PO_4$, pH 9). The resultant IMV pellet was further purified by sucrose density gradient velocity sedimentation in an ultracentrifuge (SW28 rotor). Virus bands were collected, and the virus was recovered by centrifugation in phosphate-buffered saline (PBS) ($10^7$ PFU per ml).

**Lipid/PDA vesicles.** 10,12-Tricosadiynoic acid (the diacetylene monomer) was dissolved in chloroform and filtered through a 0.45-μm filter prior to use. Mixtures containing lipids (DMPE, Sph, Chl, DMPG, and DMPC and their combinations) and the diacetylene monomer at molar ratios of 1:1:3 (DMPE/DMPG/PDA vesicles or Sph/Chl/PDA vesicles) or 2:3 (DMPC/PDA vesicles or Sph/PDA vesicles) were diluted in chloroform and dried in vacuum. The dry films of lipid/monomer mixtures were probe sonicated in deionized water at 70°C. The vesicle solution was then cooled and kept at 4°C overnight. The total lipid concentration of the DMPE/DMPG/PDA vesicle solution was 7.3 mM, while in DMPC/PDA, Sph/PDA, and Sph/Chl/PDA vesicles, the lipid concentrations were all 1 mM.

**Preparation of PDA-labeled cells.** Cells were harvested by EDTA-PBS treatment and washed in HEPES buffer (20 mM HEPES, 137 mM NaCl, 2.7 mM KCl, 1 mM $KH_2PO_4$, 5 mM D-glucose, pH 7.4) by centrifugation at 400 × *g* for 7 min. DMPE/DMPG/PDA vesicles (final lipid concentration of 0.4 mM) were added to the cells at a density of $1 \times 10^6$ cells per 1 ml buffer and incubated for 30 min with slow shaking. Following incubation, the cell suspension was irradiated at 254 nm to achieve polymerization of PDA, which resulted in a blue appearance to the cell suspension. The vesicle/cell hybrids were washed three times for removal of nonassociated vesicles and resuspended in the buffer before conducting measurements. All experimental steps were carried out at 25°C. Cell viability after treatment was not less than 90% as determined by the trypan blue exclusion assay.

**PDA fluorescence measurements.** Steady-state emission spectra were acquired at 25°C with a FL920 spectrofluorimeter (Edinburgh Co., Edinburgh, United Kingdom) using excitation at 485 nm and emission at 563 nm. Excitation and emission slits were both 10 nm. All samples were placed in a quartz cell having a 0.5-cm optical path length. Light scattering in all samples was confirmed to account for less than 5% of the fluorescence emission intensity.

Vesicles preincubated in HEPES buffer for 30 min (50/50 [vol/vol]) and irradiated for 10 to 20 seconds at 254 nm to polymerize the polydiacetylene backbone were mixed with VV, and the total volume was adjusted to 1 ml (final concentrations were 30 μM for total lipids and $0.25 \times 10^6$ PFU per ml of VV). The net fluorescence intensities (accounting for the control fluorescence from the same volume without VV present) were reported as percentages compared to the maximal PDA fluorescence, obtained by heating the lipid/PDA vesicles to produce the highly fluorescent red PDA phase.

In the experiments monitoring EGF hormone effects using PDA-labeled cells, sample volumes were 1 ml, containing $2 \times 10^6$ cells. The cells, with or without EGF pretreatment, were mixed with VV at a multiplicity of infection (MOI) of 1 PFU/cell with continous stirring. Parallel fluorescence measurements were carried out in mock infection conditions.

**Fluorescence resonance energy transfer (FRET).** Vesicles prepared according to the procedure described in "Lipid/PDA vesicles" above were additionally supplemented by *N*-NBD-PE and *N*-Rh-PE at a 100:1 (phospholipid:fluorophore) molar ratio. Vesicle solutions containing 30 μM total lipids were used in 1 ml buffer. Emission spectra were acquired in 530 nm (for *N*-NBD-PE) and 585 nm (for *N*-Rh-PE) (excitation, 469 nm) at 25°C on a FL920 spectrofluorimeter in the presence of VV at $0.25 \times 10^6$ PFU per ml. The extent of fusion was determined by the equation (3) % Fusion = $[(R_f - R_i)/(R_t - R_i)] \times 100$, where $R$ corresponds to the fluorescence emission of NBD (530 nm)/Rh (585 nm). The indices $i$, $f$, and $t$ correspond to initial, final, and following the addition of 10% Triton X-100 (a detergent causing maximum dispersion of fluorescence lipid dyes), respectively.

**Steady-state fluorescence anisotropy.** The fluorescence probe TMAP-DPH was added to the polymerized lipid/PDA vesicles, prepared as explained above, up to a final concentration of 0.1 μM (phospholipid:dye ratio of approximately 400:1). The vesicle solutions containing the fluorescent probe were allowed to equilibrate for around 30 min before the addition of VV ($0.25 \times 10^6$ PFU per ml) or PBS (mock infection). Fluorescence anisotropy was measured at 430 nm (excitation at 356 nm) on a FL920 spectrofluorimeter and calculated by conventional methodology (28). All experiments were conducted in ratio mode in which the anisotropy was measured against a control (liposomes with embedded DPH). Contribution of light scattering to fluorescence intensity was confirmed to be less than 5%.

**Fluorescence quenching.** NBD-PE was added to phospholipids in 1 mol% prior to sonication. The vesicles reacted with VV ($0.25 \times 10^6$ PFU per ml) or the same volume of PBS (mock infection). The fluorescence quenching reaction was initiated by adding sodium dithionite from a 0.6 M stock solution prepared in 50 mM Tris-base buffer (pH 11) to a final concentration of 10 mM. The decrease in fluorescence was recorded for 10 min at 25°C using 467-nm excitation and 530-nm emission on a FL920 spectrofluorimeter. The fluorescence decay is reported as a percentage of the initial fluorescence measured before the addition of dithionite.

**Confocal laser microscopy.** CHO cells were seeded on glass coverslips in 24-well plates. Cells were washed out from growth medium and incubated with HEPES buffer containing DMPE/DMPG/PDA liposomes (final lipid concentration of 0.4 mM) for 30 min under slow shaking. Following incubation, the vesicle/cell hybrids were washed three times for removal of nonbound vesicles, incubated for an additional 30 minutes in serum- and phenol red-free medium at 25°C, and irradiated for 20 seconds at 254 nm to induce PDA polymerization. The cells were infected with VV at an MOI of 10 PFU per cell. All steps were carried out at 25°C. Fluorescence images of the cells were acquired on a laser-scanning confocal microscope Axiovert-100 M (Zeiss, Germany) with a Plan-Neofluar 100×/1.3 oil objective. Excitation was 488 nm using an argon laser source. Emitted light was collected through a band-pass 625- to 655-nm filter.

## RESULTS

**Vaccinia virus interactions with lipid/PDA vesicles.** An important question this study aims to address concerns the dependence of membrane interactions of VV upon bilayer makeup and organization. In that regard, the lipid composition of the chromatic lipid/PDA vesicle platform can be easily varied (25). Figures 2 to 5 present experimental results designed to evaluate the extent of bilayer binding, penetration, and membrane fusion of vaccinia virus and examine the relationship between these parameters and lipid constituents in the bilayer. Importantly, the experiments depicted in Fig. 2 to 5 were not designed to address internalization of virions, since the overall sizes of the viral particles and vesicles are comparable.

**Virus-lipid binding.** To gain insight into the extent of binding and penetration of the viral envelope into membrane bilayers, we created lipid/PDA vesicles containing different lipid compositions and examined their chromatic response to the viral particles (Fig. 2). In the experiment depicted in Fig. 2A, we measured the intensities of fluorescence emission (excitation at 485 nm, emission at 563 nm) and kinetic profiles of the fluorescence induced following interactions between VV and the lipid/PDA vesicles. Figure 2A demonstrates significant differences in the extent and time dependence of the fluorescence signals induced by the virus within the lipid/PDA vesicles. Specifically, the highest (and steepest) fluorescence emission was induced by VV interacting with DMPC/PDA vesicles, lower fluorescence was apparent after the addition of virus particles to sphingomyelin/PDA, while the slowest increase in fluorescence up to a relatively low emission level was observed in the case of sphingomyelin/cholesterol/PDA (Fig. 2A).

The different fluorescence responses of the lipid/PDA vesicles can be explained according to the model depicted in Fig. 2B. In particular, it should be emphasized that the fluorescence emission from the PDA matrix is directly related to structural perturbations of the pendant side chains of the polymer, primarily through surface interactions (13, 40). Specifically, previous studies have shown that a rapid phase transformation of the conjugated network of polymer can be induced by external analytes physically bound to the lipid/PDA interface (13). Such interactions generally give rise to enhanced surface pressures within the model vesicles, consequently affecting the structural (and chromatic) transitions. Accordingly, the steep fluorescence increase in the case of the DMPC/PDA vesicles points to the occurrence of significant binding of the virus particles to the polymer surface, rather than insertion into the DMPC domains. On the other hand, affinity and penetration of the viral envelope into the lipid bilayers, rather than binding the PDA polymer, are the likely scenario in the case of the sphingomyelin/cholesterol/PDA vesicles, which accounts for the low fluorescence emission (induced through local perturbations of polymer domains adjacent to the lipid moieties). Indeed, recent studies have identified vaccinia virus envelope proteins which specifically target sphingomyelin/cholesterol domains within the host-cell membrane that promote viral internalization (12).

The results of fluorescence anisotropy analysis, depicted in Fig. 3, also point to the greater affinity of VV to sphingomyelin/cholesterol domains. The experiments summarized in Fig. 3 show the changes induced by VV in the fluorescence anisotropy of the dye TMAP-DPH (33) incorporated into the lipid/PDA vesicles. In these experiments, DPH was anchored within the lipid moieties by the hydrophobic TMAP residue, thus constituting a sensitive probe for changes in the fluidity within the lipid bilayer environment (17). In particular, the greater mobility of the bilayer-embedded DPH dye would produce less

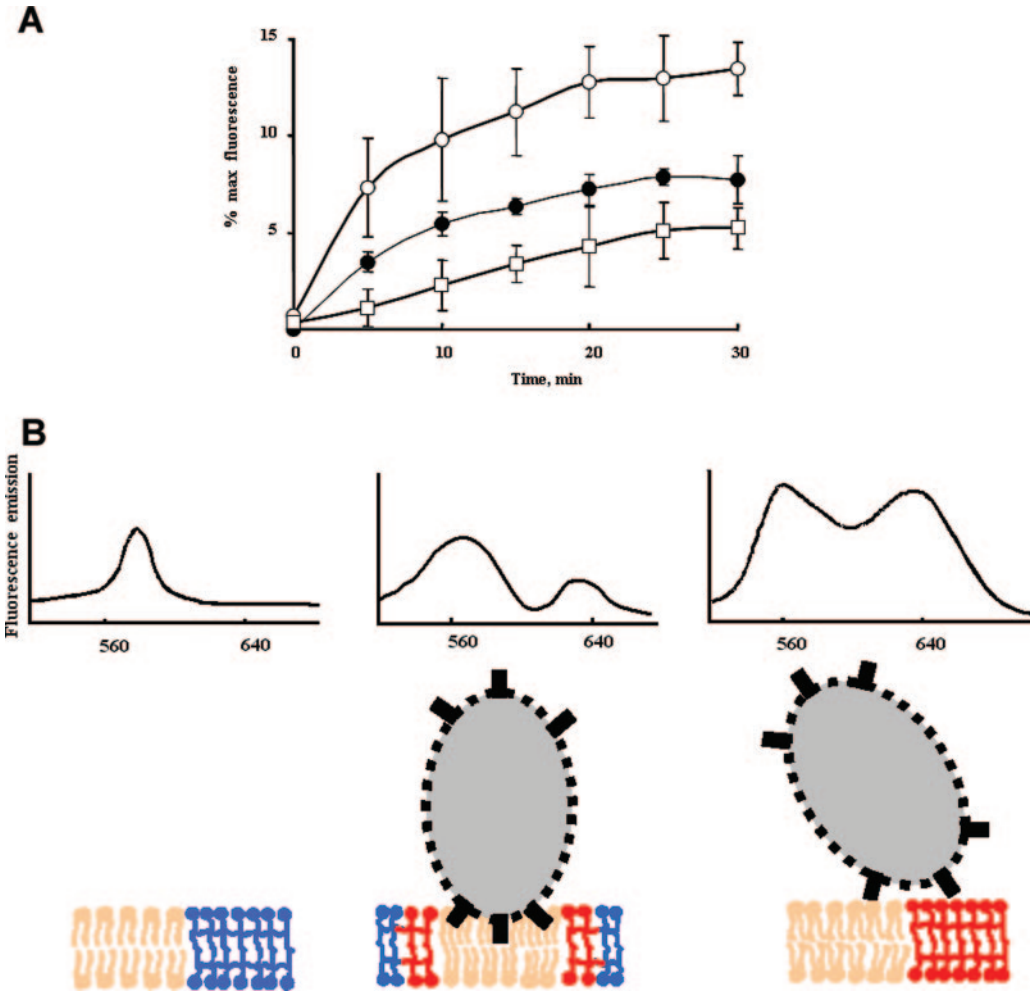


FIG. 2. VV interactions with chromatic vesicles containing PDA and different lipids. (A) Kinetic dose-response curves of PDA fluorescence, emitted from vesicles having different lipid compositions after the addition of VV ($0.25 \times 10^6$ PFU per ml). The fluorescence values are shown as percentages of the maximal (max) PDA fluorescence of red-phase PDA. DMPC/PDA (2:3 mol ratio) (empty circles), sphingomyelin/PDA (2:3) (filled circles), and sphingomyelin/cholesterol/PDA (1:1:3) (squares) are shown. Data points shown are the means ± standard deviations (error bars) ($n = 4$). (B) Schematic models depicting the relationship between bilayer penetration and fluorescence transitions. (Left) Initial unperturbed vesicle bilayer (lipids [beige]; PDA[blue]). (Middle) Penetration of viral envelope into the lipid bilayer induces local disruption of adjacent polymer domains and low fluorescence emission. (Right) Binding of viral particles to the vesicle surface induces substantial perturbation of PDA and high fluorescence.

fluorescence anisotropy, while a more restricted environment gives rise to higher anisotropy (17).

Indeed, the bar diagram in Fig. 3 demonstrates that VV interaction with the TMAP-DPH/sphingomyelin/cholesterol/PDA vesicles gave rise to a significant increase in the DPH anisotropy. The higher anisotropy of the dye is indicative of a reduced lipid mobility that can be explained by tight viral binding onto the lipid bilayers. In contrast to the pronounced effect of VV on the DPH fluorescence anisotropy in the case of TMAP-DPH/sphingomyelin/cholesterol/PDA, virus addition to DMPC/PDA or sphingomyelin/PDA vesicles that further incorporated TMAP-DPH hardly had an effect, reflecting the lesser affinity and binding of the viral particles into the lipid domains in those vesicles.

The fluorescence quenching data depicted in Fig. 4 portray a similar picture with regard to the relationship between the lipid composition of the membrane and viral interactions. In the experiment featured in Fig. 4, we prepared lipid/PDA vesicles having different lipid compositions that additionally incorporated the fluorescence dye NBD-PE. This fluorescence marker is anchored in the lipid bilayer through the PE moiety, with the NBD protruding at the bilayer surface. This configuration facilitates gradual, time-dependent quenching of the dye's fluorescence, occurring for example after dissolving sodium dithionite (a fluorescence quencher) in the aqueous solution containing the vesicles (10). The quenching rate, however, can be affected by masking of the fluorescence dye by vesicle-bound species, making the NBD-PE system a powerful probe for evaluation of binding and surface occupation in vesicle systems (26).

Figure 4 demonstrates a clear dependence of the NBD quenching rate on the lipid composition of the vesicles when VV was added prior to the quencher. Specifically, the quenching rates of NBD-PE/DMPC/PDA and NBD-PE/sphingomy-

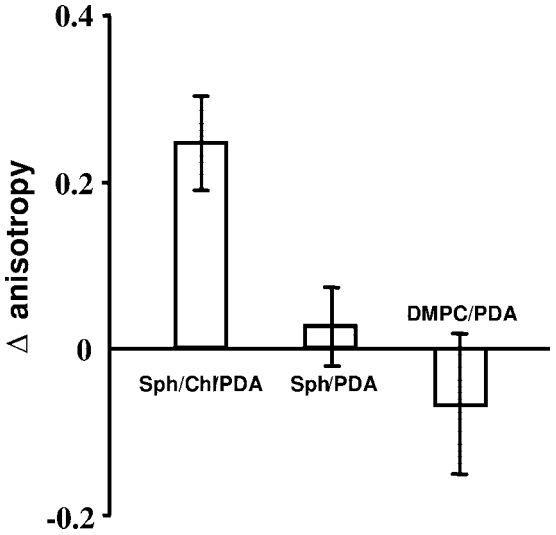


FIG. 3. Effect of VV on lipid fluidity. Changes of fluorescence anisotropy of vesicle-incorporated TMAP-DPH induced by the addition of VV particles ($0.25 \times 10^6$ PFU per ml). Data shown are means ± standard deviations (error bars) of four independent experiments.

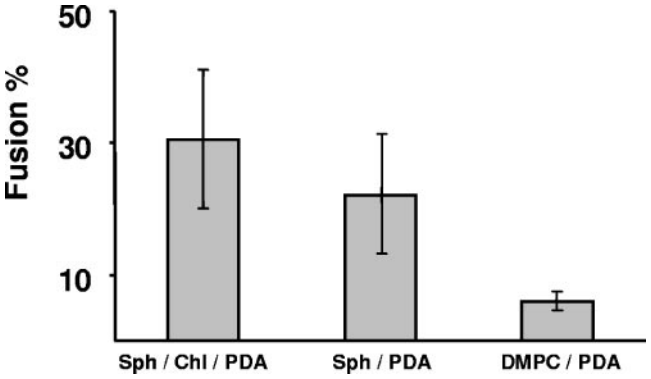


FIG. 5. FRET analysis of fusion between vaccinia virus envelope and lipid/PDA vesicles. Lipid/PDA vesicles (the specific lipid composition is indicated below each bar) supplemented by *N*-NBD-PE and *N*-Rh-PE at a 100:1 (phospholipid:fluorophore) molar ratio were incubated with VV ($0.25 \times 10^6$ PFU per ml) at 25°C for 20 min. Data are shown as mean values ± standard deviations (error bars) ($n = 4$). Energy transfer between donor and acceptor is reduced if significant fusion occurs between the vesicles containing the fluorescence dyes and unlabeled virus envelope.

elin/PDA were not affected by the preaddition of VV (Fig. 4A and B). (The insignificant quenching of NBD-PE incorporated within sphingomyelin/PDA vesicles [Fig. 4B] is probably due to localization of the dye in the inner leaflet of these vesicles [4]). However, when VV was added to NBD-PE/sphingomyelin/cholesterol/PDA vesicles prior to dithionite, the effect on the quenching rate was significant: very little quenching was apparent after VV addition compared to the quenching rate recorded when no virus was added (Fig. 4C). The dramatic inhibition of fluorescence quenching most likely corresponds to the attachment and insertion of the virus envelope into the vesicle bilayer, thereby "masking" the NBD from the water-dissolved quencher.

**Viral fusion with lipid bilayers.** To complement the data in Fig. 2 to 4 indicating a preferred binding and insertion of the viral particles into lipid bilayers comprising sphingomyelin and cholesterol, we further carried out fluorescence resonance energy transfer experiments designed to evaluate the degree of insertion and fusion between the viral envelope and the lipid/PDA vesicles (Fig. 5). In the FRET experiments, we prepared vesicles comprising PDA, different lipids (DMPC, sphingomyelin, or sphingomyelin/cholesterol), and fluorescent dyes: phospholipids displaying the fluorescence energy donor *N*-NBD-PE and also lipids onto which the fluorescence acceptor *N*-Rh-PE was attached (42). FRET analysis measures the energy transfer between donor and acceptor. In the case of the intact and isolated vesicles in aqueous solutions, high-energy transfer is recorded due to the relative close proximity between the donor and acceptor molecules. However, if the fluorescently labeled vesicles undergo fusion with unlabeled species (other vesicles, cell membrane, or viral envelope), the donor and acceptor compounds are dispersed within the fused particles, resulting in reduced energy transfer due to the greater average distance between the fluorescent markers. Specifically, the extent of fusion between the *N*-NBD-PE/*N*-Rh-PE/lipid/PDA vesicles and the virus particles can be calculated (as per-

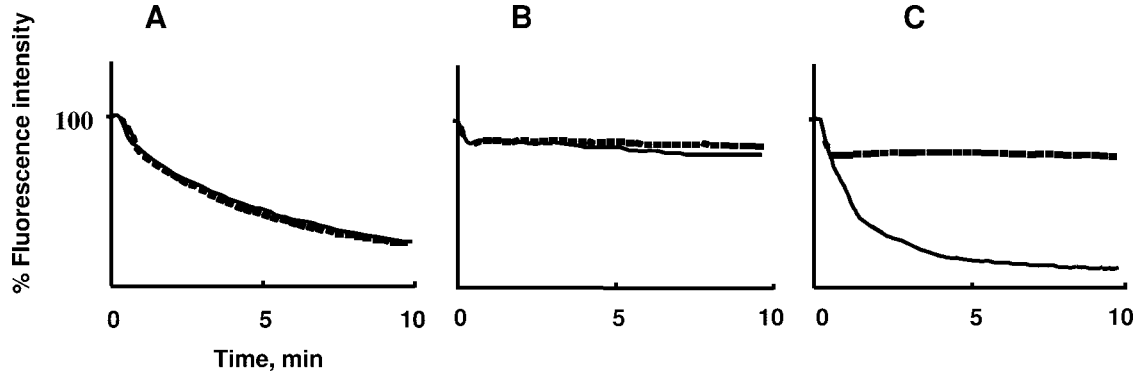


FIG. 4. Effects of VV interactions on the fluorescence quenching of vesicle-incorporated NBD-PE. Quenching rates of NBD-PE by sodium dithionite and the effect of vaccinia virus added prior to the quencher are shown. Solid curves, NBD quenching in the control vesicle solutions (without the addition of virus); broken curves, decay of fluorescence in the presence of vaccinia virus ($0.25 \times 10^6$ PFU per ml). DMPC/PDA (A), sphingomyelin/PDA (B), and sphingomyelin/cholesterol/PDA (C) vesicles were used.

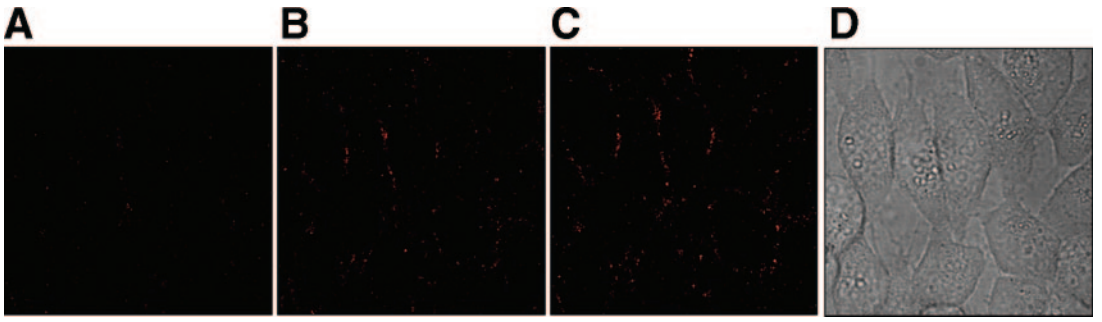


FIG. 6. Confocal fluorescence microscopy of VV interactions with the membranes of PDA-labeled cells. Fluorescence microscopy images (excitation 485 nm, emission 625 to 655 nm) were recorded at different time intervals (5 min [A], 20 min [B], and 30 min [C]) after the PDA-labeled CHO cells were mixed with vaccinia virus particles at 25°C (MOI of 10 PFU per cell). (D) Transmission image of the same cells.

centages) from the ratios of the fluorescence peaks of the donor and acceptor (3).

Similar to the data depicted in Fig. 2 to 4, the FRET data showed significant dependence upon the lipid composition of the vesicles. In particular, the low fusion recorded following the addition of VV to the DMPC/PDA vesicles (less than 10% [Fig. 5]) stands in contrast to the situation encountered in sphingomyelin/PDA vesicles (approximately 25% fusion) and in sphingomyelin/cholesterol/PDA vesicles (around 30%). This result corroborates the primary roles of sphingomyelin and particularly sphingomyelin/cholesterol domains in promoting VV-vesicle fusion (12). The fluorescence data depicted in Fig. 5 are consistent with the interpretation of the chromatic and analytical data in Fig. 2 to 4; binding and penetration of the virus particles into the sphingomyelin/cholesterol domains can explain the higher degree of fusion apparent in the FRET experiments. In contrast, less interaction of VV with the phospholipids encountered in the DMPC/PDA vesicles is not expected to produce significant lipid fusion as is shown in Fig. 5.

**Vaccinia virus interactions with PDA-labeled CHO cells.** While Fig. 2 to 5 feature experiments designed to probe viral interactions with model vesicle systems, we further investigated the effects of virus binding to the plasma membrane of living cells using PDA-labeled CHO cells (Fig. 6 and 7). This analysis was based on the recent discovery that PDA nanopatches can be incorporated into the plasma membranes of live cells, thereby allowing real-time spectroscopy and microscopy analysis of membrane processes in the actual membrane environment (31, 38). Particularly important in the context of this study, PDA-labeled cells provide useful information on local structural perturbations within the cell membrane.

Labeling of CHO cells with DMPE/DMPG/PDA vesicles (1:1:3 mol ratio) was achieved through incubating the lipid/PDA vesicles with the cells in HEPES buffer for 30 min. The choice of this particular phospholipid composition yielded an optimal coverage of the CHO surfaces with PDA patches. Microscopy analysis (data not shown) confirmed that the CHO cells maintained their normal shape following PDA treatment and that their viability was not adversely affected through the duration of the experiment. Microscopy experiments further detected (data not shown) cytopathological consequences of virus-infected PDA-labeled cells that were identical to those of unlabeled cells, indicating the minimal perturbation to the cell by PDA labeling.

**Confocal laser microscopy.** PDA-labeled cells were employed for investigating the surface localization and progression of VV attachment to the CHO cell membrane using confocal fluorescence microscopy (excitation 485 nm, emission 625 to 655 nm [Fig. 6]). The microscopy images correspond to a single slice in the horizontal monolayer plan extracted from the cell assembly. Accordingly, the fluorescent PDA nanopatches appear on the cell borders, due to PDA localization at the cell membrane. The important observation apparent from the microscopy images in Fig. 6 is that viral attachment to the membrane is a gradual rather than instantaneous process. Specifically, Fig. 6A shows that hardly any fluorescence was emitted from the membrane-incorporated PDA patches a short time after virus addition, indicating that no significant bilayer perturbation took place at that stage. However, fluorescent PDA domains clearly appeared within the same cell membrane 20 min after the viral particles and cells were mixed (Fig. 6B), becoming more abundant and intense 30 min after virus addition (Fig. 6C). The PDA fluorescence intensities of the PDA

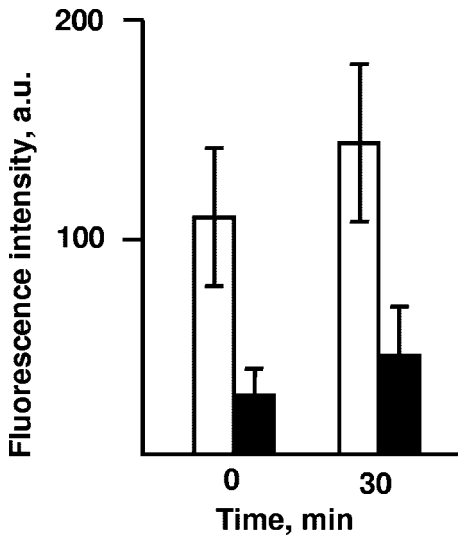


FIG. 7. Role of the EGF receptor in viral binding. Fluorescence of PDA-labeled cells incubated with VV at a low MOI (1 PFU per cell) without EGF treatment (empty bars) and after receptor saturation by EGF (2 μg/ml) (filled bars). Net fluorescence values, after subtraction of background emission (induced by mock infection), are shown.

patches remained approximately constant beyond the 30-min period (data not shown).

**Significance of EGF receptor-mediated viral uptake.** To further elucidate the mechanism of viral attachment to the cell surface and the significance of lipid binding compared to receptor-mediated membrane insertion, we examined the role of the epidermal growth factor receptor as a target for virus binding (Fig. 7). The important contribution of the EGF receptor to viral entry and for propagation of VV infection has been previously reported (23); however, several studies indicated that this receptor is not an essential determinant in the infection pathway (15, 41).

Figure 7 depicts the net fluorescence emission induced by VV interactions (at a low MOI of 1 PFU per cell) in PDA-labeled CHO cells without receptor saturation by the EGF hormone and following receptor saturation (2 μg/ml EGF hormone) (32). The fluorescence emission recorded in Fig. 7 corresponds to the chromatic transformations of the PDA nanopatches, induced by viral particles interacting with the cell membrane. Two important observations in Fig. 7 should be emphasized. First, the addition of the EGF hormone clearly attenuated the fluorescence signal from the membrane-incorporated PDA patches (Fig. 7). This result indicates that the EGF hormone reduces membrane binding of the vaccinia virus particles through blocking the receptor sites. However, Fig. 7 also demonstrates that even when the EGF receptor was saturated with the hormone, viral binding to the cell membrane still occurred (giving rise to the net PDA fluorescence). Overall, the data presented in Fig. 7 suggest that membrane binding that is not receptor mediated might still play a role in VV internalization and propagation.

## DISCUSSION

Deciphering the mechanisms by which viruses gain entry into the host cell is critical for understanding the infection process and development of therapeutic solutions. The objective of this study was to evaluate the lipid bilayer interactions of vaccinia virus and their significance within the complex viral infection process. In particular, elucidating the initial steps of viral entry prior to internalization of the viral particles into the host cells would make a significant contribution to understanding the entire infection cascade.

The analysis employed new chromatic vesicles and cell assays and specifically focused on the kinetics of viral attachment to the cell surface, the dependence of virus interactions with the cell membrane upon lipid composition, and the contributions of non-receptor-mediated pathways to virus infection. Importantly, this work has focused on bilayer interactions of VV, rather than viral internalization or the entire infection process. Indeed, the high ratio between viral particles and PFU of approximately 50:1 (44) suggests that membrane binding by itself does not guarantee viral internalization and eventual infectivity.

An important goal in this study has been to understand the mechanisms of non-receptor-mediated internalization of VV and the dependence of viral binding and membrane insertion upon lipid composition of the bilayer. Previous studies suggested that the penetration of VV into host cells involves more than one mechanism (12, 14, 19), a hypothesis that is supported by the complexity of the VV particle, which displays more than 30 different polypeptides on its envelope (29). The experimental data summarized in Fig. 2 to 5 emphasized the pronounced effects of lipid composition on binding, insertion, and fusion of the viral envelope to the cell membrane. Fluorescence emission from lipid/PDA vesicles shown in Fig. 2 indicates that sphingomyelin/cholesterol domains promoted binding and insertion of the viral envelope into the membrane, while VV exhibited much lower affinity to DMPC. This result echoes several reports pointing to the prominent roles of membrane domains rich in sphingomyelin/cholesterol, also known as "lipid rafts," in VV internalization (12). Lipid rafts have been proposed to constitute important mediators for membrane binding and internalization in other virus species as well (5, 34, 43).

Experiments utilizing complementary bioanalytical methods (Fig. 3 to 5) corroborated the results of the chromatic lipid/PDA vesicle assay and provided further insight into viral interactions and fusion with the lipid bilayer. Specifically, fluorescence anisotropy (Fig. 3) and fluorescence quenching (Fig. 4) analyses confirmed that sphingomyelin/cholesterol domains promoted VV binding to the bilayer. Similarly, FRET analysis pointed to significantly higher fusion between the virions and lipid bilayers containing sphingomyelin/cholesterol domains (Fig. 5). In all experiments, significant differences were observed between viral binding to DMPC compared to sphingomyelin/cholesterol.

Indeed, the significance of cholesterol in promoting viral binding and insertion into the lipid bilayer is apparent in Fig. 2 to 5. These results reflect the observations that cholesterol is the core constituent of lipid rafts (6) and the adverse effects of cholesterol depletion on such rafts (16, 36). Overall, the experimental results depicted in Fig. 2 to 5 provide evidence for the dependence of VV binding, insertion, and membrane fusion upon lipid composition, particularly the presence of sphingomyelin/cholesterol domains within the bilayer. The data further suggest that IMV binding and insertion into the lipid rafts are initial steps in the fusion process.

CHO cells labeled with lipid/PDA patches yielded additional insight into the time dependence and structural consequences of viral binding to the cell surface. The experiments in which we employed the PDA-labeled cells were aimed at probing the kinetics of viral binding to the cell membrane (Fig. 6) and the putative effect of the EGF receptor upon viral binding (Fig. 7). Specifically, confocal microscopy revealed that viral binding progressed slowly, with maximal membrane binding occurring after approximately 30 min (Fig. 6). Analysis of fluorescence emission from PDA-labeled cells pretreated with EGF hormone (Fig. 7) revealed that VV binding to the host cell membrane depends to a large extent upon EGF receptor-mediated pathways. However, the experimental results also showed that host infection does not occur solely through binding to EGF receptors on the cell surface but is also promoted through additional (or simultaneous) routes involving lipid bilayer binding. Importantly, our data also demonstrate that VV surface penetration occurs at a temperature of 25°C, not only at the previously studied 37°C (12). Overall, the data recorded in real cell-membrane environments rather than model lipid bilayers add a key dimension to the study, complementing the

vesicle analysis and connecting it to virus-membrane binding processes in actual cellular environments.

In conclusion, this study provides a comprehensive analysis of VV interactions with the plasma membrane and the factors affecting viral attachment, fusion, and internalization. The experiments yielded information on the binding events, their kinetic profiles, and structural consequences. In particular, the chromatic vesicle and cell assays indicate that viral binding to the membrane bilayer is a pronounced event in the infection cascade, promoted by different lipid constituents within the cell membrane, and is also affected by putative receptor molecules embedded in the cell surface. Furthermore, this study demonstrates the potential use of the new PDA platform for studying viral infections. Overall, this work points to the existence of different pathways for viral binding and penetration into host cell targets, underlying possible mechanisms for cross-species infections.

## ACKNOWLEDGMENTS

R.J. is grateful to the Human Frontiers Science Program for generous financial support.

We are grateful to M. Tashker and E. Hahiashvily for assistance with viral purification.

## REFERENCES

1. **Appleyard, G., A. J. Hapel, and E. A. Boulter.** 1971. An antigenic difference between intracellular and extracellular rabbitpox virus. J. Gen. Virol. **13:** 9–17.
2. **Armstrong, J. A., D. H. Metz, and M. R. Young.** 1973. The mode of entry of vaccinia virus into L cells. J. Gen. Virol. **21:**533–537.
3. **Arvinte, T., and P. L. Steponkus.** 1988. Characterization of the pH-induced fusion of liposomes with the plasma membrane of rye protoplasts. Biochemistry **27:**5671–5677.
4. **Balch, C., R. Morris, E. Brooks, and R. G. Sleight.** 1994. The use of N-(7-nitrobenz-2-oxa-1,3-diazole-4-yl)-labeled lipids in determining transmembrane lipid distribution. Chem. Phys. Lipids **70:**205–212.
5. **Bavari, S., C. M. Bosio, E. Wiegand, G. Ruthel, A. B. Will, T. W. Geisbert, M. Hevey, C. Schmaljohn, A. Schmaljohn, and M. J. Aman.** 2002. Lipid raft microdomains: a gateway for compartmentalized trafficking of Ebola and Marburg viruses. J. Exp. Med. **195:**593–602.
6. **Brown, D. A., and E. London.** 2000. Structure and function of sphingolipid- and cholesterol-rich membrane rafts. J. Biol. Chem. **275:**17221–17224.
7. **Chang, A., and D. H. Metz.** 1976. Further investigations on the mode of entry of vaccinia virus into cells. J. Gen. Virol. **32:**275–282.
8. **Chang, W., J. C. Hsiao, C. S. Chung, and C. H. Bair.** 1995. Isolation of a monoclonal antibody which blocks vaccinia virus infection. J. Virol. **69:**517–522.
9. **Charych, D., Q. Cheng, A. Reichert, G. Kuziemko, M. Stroh, J. O. Nagy, W. Spevak, and R. C. Stevens.** 1996. A 'litmus test' for molecular recognition using artificial membranes. Chem. Biol. **3:**113–120.
10. **Chattopadhyay, A., and E. London.** 1987. Parallax method for direct measurement of membrane penetration depth utilizing fluorescence quenching by spin-labeled phospholipids. Biochemistry **26:**39–45.
11. **Chung, C.-S., J.-C. Hsiao, Y.-S. Chang, and W. Chang.** 1998. A27L protein mediates vaccinia virus interaction with cell surface heparan sulfate. J. Virol. **72:**1577–1585.
12. **Chung, C.-S., C.-Y. Huang, and W. Chang.** 2005. Vaccinia virus penetration requires cholesterol and results in specific viral envelope proteins associated with lipid rafts. J. Virol. **79:**1623–1634.
13. **Dobrosavljevic, V., and R. M. Stratt.** 1987. Role of conformational disorder in the electronic structure of conjugated polymers: substituted polydiacetylenes. Phys. Rev. B **35:**2781–2795.
14. **Doms, R. W., R. Blumenthal, and B. Moss.** 1990. Fusion of intra- and extracellular forms of vaccinia virus with the cell membrane. J. Virol. **64:** 4884–4892.
15. **Eppstein, D. A., Y. V. Marsh, A. B. Schreiber, S. R. Newman, G. J. Todaro, and J. J. Nestor, Jr.** 1985. Epidermal growth factor receptor occupancy inhibits vaccinia virus infection. Nature **318:**663–665.
16. **Hao, M., S. Mukherjee, and F. R. Maxfield.** 2001. Cholesterol depletion induces large scale domain segregation in living cell membranes. Proc. Natl. Acad. Sci. USA **98:**13072–13077.
17. **Ho, C., and C. D. Stubbs.** 1997. Effect of n-alkanols on lipid bilayer hydration. Biochemistry **36:**10630–10637.
18. **Hollinshead, M., A. Vanderplasschen, G. L. Smith, and D. J. Vaux.** 1999. Vaccinia virus intracellular mature virions contain only one lipid membrane. J. Virol. **73:**1503–1517.
19. **Hsiao, J. C., C. S. Chung, and W. Chang.** 1999. Vaccinia virus envelope D8L protein binds to cell surface chondroitin sulfate and mediates the adsorption of intracellular mature virions to cells. J. Virol. **73:**8750–8761.
20. **Janeczko, R. A., J. F. Rodriguez, and M. Esteban.** 1987. Studies on the mechanism of entry of vaccinia virus in animal cells. Arch. Virol. **92:**135–150.
21. **Joklik, W. K.** 1962. The purification for four strains of poxvirus. Virology **18:**9–18.
22. **Katz, M., I. Ben-Shlush, S. Kolusheva, and R. Jelinek.** 2006. Rapid colorimetric screening of drug interaction and penetration through lipid barriers. Pharm. Res. **23:**580–588.
23. **King, C. S., J. A. Cooper, B. Moss, and D. R. Twardzik.** 1986. Vaccinia virus growth factor stimulates tyrosine protein kinase activity of A431 cell epidermal growth factor receptors. Mol. Cell. Biol. **6:**332–336.
24. **Kobayashi, T., M. Yasuda, S. Okada, H. Matsuda, and H. Nakanishi.** 1997. Femtosecond spectroscopy of a polydiacetylene with extended conjugation to acetylenic side groups. Chem. Phys. Lett. **267:**472–480.
25. **Kolusheva, S., E. Wachtel, and R. Jelinek.** 2003. Biomimetic lipid/polymer colorimetric membranes: molecular and cooperative properties. J. Lipid Res. **44:**65–71.
26. **Kolusheva, S., J. Friedman, I. Angel, and R. Jelinek.** 2005. Membrane interactions and metal ion effects on bilayer permeation of the lipophilic ion modulator DP-109. Biochemistry **44:**12077–12085.
27. **Kolusheva, S., T. Shahal, and R. Jelinek.** 2000. Peptide-membrane interactions studied by a new phospholipid/polydiacetylene colorimetric vesicle assay. Biochemistry **39:**15851–15859.
28. **Kolusheva, S., T. Shahal, and R. Jelinek.** 2000. Cation-selective color sensors composed of ionophore-phospholipid-polydiacetylene mixed vesicles. J. Am. Chem. Soc. **122:**776–780.
29. **Oie, M., and Y. Ichihashi.** 1981. Characterization of vaccinia polypeptides. Virology **113:**263–276.
30. **Okada, S., S. Peng, W. Spevak, and D. Charych.** 1998. Color and chromism of polydiacetylene vesicles. Acc. Chem. Res. **31:**229–239.
31. **Orynbayeva, Z., S. Kolusheva, E. Livneh, A. Lichtenshtein, I. Nathan, and R. Jelinek.** 2005. Visualization of membrane processes in living cells by surface-attached chromatic polymer patches. Angew. Chem. Int. Ed. Engl. **44:**1092–1096.
32. **Ozcan, F., P. Klein, M. A. Lemmon, I. Lax, and J. Schlessinger.** 2006. On the nature of low- and high-affinity EGF receptors on living cells. Proc. Natl. Acad. Sci. USA **103:**5735–5740.
33. **Parente, R. A., and B. R. Lentz.** 1985. Advantages and limitations of 1-palmitoyl-2-[[2-[4-(6-phenyl-trans-1,3,5-hexatrienyl)phenyl]ethyl]carbonyl]-3-sn-phosphatidylcholine as a fluorescent membrane probe. Biochemistry **24:** 6178–6185.
34. **Popik, W., T. M. Alce, and W. C. Au.** 2002. Human immunodeficiency virus type 1 uses lipid raft-colocalized CD4 and chemokine receptors for productive entry into $CD4^+$ T cells. J. Virol. **76:**4709–4722.
35. **Ringsdorf, H., B. Schlarb, and J. Venzmer.** 1988. Molecular architecture and function of polymeric oriented systems: models for study of organization, surface recognition, and dynamics of biomembranes. Angew. Chem. **27:**113–158.
36. **Rothberg, K. G., Y. S. Ying, B. A. Kamen, and R. G. Anderson.** 1990. Cholesterol controls the clustering of the glycophospholipid-anchored membrane receptor for 5-methyltetrahydrofolate. J. Cell Biol. **111:**2931–2938.
37. **Rozner, S., S. Kolusheva, Z. Cohen, W. Dowhan, J. Eichler, and R. Jelinek.** 2003. Detection and analysis of membrane interactions by a biomimetic colorimetric lipid/polydiacetylene assay. Anal. Biochem. **319:**96–104.
38. **Shtelman, E., A. Tomer, S. Kolusheva, and R. Jelinek.** 2006. Imaging membrane processes in erythrocyte ghosts by surface fusion of a chromatic polymer. Anal. Biochem. **348:**151–153.
39. **Smith, G. L., A. Vanderplasschen, and M. Law.** 2002. The formation and function of extracellular enveloped vaccinia virus. J. Gen. Virol. **83:**2915–2931.
40. **Song, J., Q. Cheng, S. Zhu, and R. C. Stevens.** 2002. "Smart" materials for biosensing devices: cell-mimicking supramolecular assemblies and colorimetric detection of pathogenic agents. Biomed. Microdevices **4:**213–221.
41. **Stroobant, P., A. P. Rice, W. J. Gullick, D. J. Cheng, I. M. Kerr, and M. D. Waterfield.** 1985. Purification and characterization of vaccinia virus growth factor. Cell **42:**383–393.
42. **Struck, D. K., D. Hoekstra, and R. E. Pagano.** 1981. Use of resonance energy transfer to monitor membrane fusion. Biochemistry **20:**4093–4099.
43. **Stuart, A. D., H. E. Eustace, T. A. McKee, and T. D. Brown.** 2002. A novel cell entry pathway for a DAF-using human enterovirus is dependent on lipid rafts. J. Virol. **76:**9307–9322.
44. **Vanderplasschen, A., and G. L. Smith.** 1997. A novel virus binding assay using confocal microscopy: demonstration that the intracellular and extracellular vaccinia virions bind to different cellular receptors. J. Virol. **71:**4032–4041.
45. **Vázquez, M. I., and M. Esteban.** 1999. Identification of functional domains in the 14-kilodalton envelope protein (A27L) of vaccinia virus. J. Virol. **73:**9098–9109.